Experimental investigation of symmetry properties of second harmonic Lamb waves

Yu Liu, Jin-Yeon Kim, Laurence J. Jacobs, Jianmin Qu, and Zheng Li

Citation: J. Appl. Phys. **111**, 053511 (2012); doi: 10.1063/1.3691225
View online: http://dx.doi.org/10.1063/1.3691225
View Table of Contents: http://jap.aip.org/resource/1/JAPIAU/v111/i5
Published by the American Institute of Physics.

Experimental investigation of symmetry properties of second harmonic Lamb waves

Yu Liu,[1,2] Jin-Yeon Kim,[2,a)] Laurence J. Jacobs,[2,3] Jianmin Qu,[4] and Zheng Li[1]
[1]*State Key Laboratory of Turbulence and Complex System and College of Engineering, Peking University, Beijing 100871, China*
[2]*School of Civil and Environmental Engineering, Georgia Institute of Technology, Atlanta, Georgia 30332-0355, USA*
[3]*Woodruff School of Mechanical Engineering, Georgia Institute of Technology, Atlanta, Georgia 30332-0405, USA*
[4]*Department of Civil and Environmental Engineering, Northwestern University, Evanston, Illinois 60208, USA*

(Received 24 October 2011; accepted 1 February 2012; published online 6 March 2012)

Recent studies by multiple authors show contradictory results concerning the symmetry properties of second harmonic Lamb waves. This research experimentally investigates this symmetry issue by examining both symmetric (s1-s2) and anti-symmetric (a1-a2 and a2-a4) mode pairs in aluminum plates under the same experimental conditions. The wedge technique is used to generate and detect ultrasonic Lamb wave signals of a specific mode, and the Morlet wavelet is applied to extract the fundamental and second harmonic amplitudes. The measured normalized second harmonic amplitudes of the three different mode pairs all show a linear increase with propagation distance. However, the slopes of the two anti-symmetric mode pairs are smaller by two to three orders of magnitude than that of the symmetric mode pair considered. Further investigations of these two anti-symmetric mode pairs for plates with different levels of material nonlinearity reveal consistently small slopes that are independent of the level of material nonlinearity. Therefore, this research experimentally demonstrates that the second harmonic generation in anti-symmetric Lamb wave modes is extremely inefficient; this result is consistent with some recent theoretical predictions and thus shows that the use of these anti-symmetric modes is not favorable for the experimental characterization of material nonlinearity. © *2012 American Institute of Physics*. [http://dx.doi.org/10.1063/1.3691225]

I. INTRODUCTION

Previous research has shown that nonlinear Lamb wave techniques can be used to characterize acoustic nonlinearity, which in turn can be an indicator of damage due to fatigue or thermal aging.[1–5] These techniques rely on the measurement of the second harmonic Lamb waves generated by the intrinsic material nonlinearity which is related to the lattice anharmonicity and/or microstructural defects such as dislocations or precipitates. Compared to nondispersive longitudinal and Rayleigh waves,[6–8] Lamb waves have the potential to be utilized to efficiently monitor damage in large plate-like structures because they can propagate relatively long distances and interrogate the entire thickness of a structure. However, their inherently dispersive and multi-modal nature introduces difficulties in measurements, making a careful theoretical analysis necessary for their application to assess material damage. One important issue is the selection of a mode pair that can efficiently generate a second harmonic wave and thus reliably characterize material nonlinearity.

Recent theoretical studies[9–12] on nonlinear Lamb waves demonstrate that only specific mode pairs that satisfy certain conditions exhibit cumulative second harmonic generation, i.e., a linear growth of the second harmonic amplitude with propagation distance. Although both phase and group velocity matching have been established as necessary conditions for cumulative second harmonic generation, there are contradictory arguments related to the symmetry properties of second harmonic Lamb waves. Deng,[9,10] Müller *et al.*,[11] and Srivastava *et al.*[12] theoretically conclude that cumulative second harmonic generation can occur only in the symmetric second harmonic modes. Symmetric mode pairs at the material's longitudinal wave velocity[13,14] (s1-s2, s2-s4) and an anti-symmetric-symmetric mode pair at the crossing points[15] (a2-s4) in the phase velocity dispersion plot have been experimentally shown to be useful in measuring material nonlinearity. In contrast, de Lima and Hamilton[16] argue that only second harmonic modes of the same symmetry as the primary modes can be generated, which implies the possibility of anti-symmetric second harmonic mode generation by an anti-symmetric primary mode. Furthermore, Lee *et al.*[17] reported experimental results on the cumulative propagation of an anti-symmetric second harmonic mode. Most recently, Matsuda and Biwa[18] analyzed the Lamb wave mode pairs that simultaneously satisfy the phase and group velocity matching conditions. By not taking the excitability condition into account, their analysis implicitly allows for the possibility of anti-symmetric second harmonic generation. Therefore, further investigation is needed in order to unravel these contradictions and provide guidance for mode selection in the applications of nonlinear Lamb waves.

a)Author to whom correspondence should be addressed. Electronic mail: jinyeon.kim@me.gatech.edu.

The objective of this research is to experimentally investigate the symmetry properties of second harmonic Lamb waves by measuring the modal responses of symmetric and anti-symmetric second harmonic Lamb wave modes. The selected mode pairs are examined for their efficiency in characterizing the inherent material nonlinearity of undamaged aluminum plates under the same experimental conditions. By carefully comparing the results for these mode pairs and then examining the anti-symmetric mode pairs in two materials with different levels of material nonlinearity, a conclusion on the symmetry properties of the second harmonic Lamb modes is reached.

II. CUMULATIVE SECOND HARMONIC GENERATION OF LAMB WAVES

This section briefly summarizes the theoretical conditions for the cumulative second harmonic generation of Lamb waves. Following the work by Müller *et al.*,[11] consider the propagation of plane time-harmonic Lamb waves in an isotropic, homogeneous, nonlinear elastic plate with stress-free boundary conditions. It is assumed that the wave motions are in the y-z plane and the wave propagation occurs in the z-direction. The total displacement field can be assumed to be the sum of a primary wave $\mathbf{u}^{(1)}$ (at frequency ω) and a second harmonic wave $\mathbf{u}^{(2)}$ (at frequency 2ω) based on the perturbation condition $|\mathbf{u}^{(2)}| \ll |\mathbf{u}^{(1)}|$. The perturbation method is applicable and well supported by experimental results, which show that the amplitude of the second harmonic wave is much smaller than that of the primary wave.[7,8,13,14] The solution for the second harmonic wave $\mathbf{u}^{(2)}$ can be written in the normal mode expansion form[9,11]

$$\mathbf{u}^{(2)}(y,z,t) = \sum_n A_n(z)\tilde{\mathbf{u}}_n^{(2)}(y)e^{-2i\omega t}, \tag{1}$$

where $A_n(z)$ is the amplitude or spatial dependence of the nth second harmonic mode $\tilde{\mathbf{u}}_n^{(2)}(y)$. Clearly, $A_n(z)$ should not vanish in order for the second harmonic wave to be generated. Its expression is given as

$$A_n(z) = \frac{f_n^{vol} + f_n^{surf}}{4P_{nn}} \begin{cases} \dfrac{i}{\kappa_n^* - 2\kappa}\left(e^{2i\kappa z} - e^{i\kappa_n^* z}\right) & \text{if } \kappa_n^* \neq 2\kappa \\ ze^{2i\kappa z} & \text{if } \kappa_n^* = 2\kappa \end{cases}, \tag{2}$$

where κ and κ_n^* (with * denoting the complex conjugate) are wave numbers of the primary mode and the nth second harmonic mode, respectively; P_{nn} is the power carried by the nth second harmonic mode; f_n^{vol} and f_n^{surf} are power fluxes from the primary mode to the second harmonic mode through the volume and surface of the plate, respectively. Detailed expressions for these terms can be found in the work of Müller *et al.*[11] Note that f_n^{vol} and f_n^{surf} act as the modal driving forces of the second harmonic mode due to the material nonlinearity.

It is seen from Eq. (2) that the second harmonic wave can be excited ($A_n(z) \neq 0$) only if the total power flux is nonzero (i.e., $f_n^{vol} + f_n^{surf} \neq 0$), which is referred to as the excitability condition for the second harmonic Lamb waves. A careful examination[11] shows that $f_n^{vol} + f_n^{surf} \neq 0$ generally holds for a symmetric second harmonic mode, whereas $f_n^{vol} + f_n^{surf} = 0$ for an anti-symmetric second harmonic mode, which means that only symmetric second harmonic Lamb wave modes can be excited. Furthermore, when $\kappa_n^* = 2\kappa$ is satisfied in Eq. (2), i.e., the phase velocity of the primary wave is equal to that of the second harmonic wave (phase velocity matching), the amplitude of the second harmonic wave grows linearly as it propagates. An additional condition, namely, group velocity matching,[1,11] is required for cumulative second harmonic generation when the primary wave is a pulse of a finite number of cycles, as is the case in most practical experiments. This means that the primary and secondary harmonic waves travel at the same group velocity; thus the energy that leaks out of the primary wave can be accumulated in the second harmonic wave. To conclude, three conditions—the nonzero power flux, phase velocity matching, and group velocity matching—should be simultaneously satisfied in order for the cumulative generation of the second harmonic Lamb waves to occur.

As mentioned in the above, the group velocity matching condition is required only due to the dispersion effect that occurs when the fundamental wave is a pulse of finite duration. The experimental technique used in this paper measures the amplitude of the naturally cumulative second harmonic mode and thus requires that the group velocity matching condition be satisfied. However, the experimental technique of Deng *et al.*[19] does not require group velocity matching. Their technique integrates the dispersed (noncumulative) second harmonic signal; the integrating operation works as an artificial accumulation of naturally noncumulative second harmonic signals, which enables the observation of an effect equivalent to the cumulative second harmonic propagation that can be observed in the naturally cumulative second harmonic mode.

III. EXPERIMENTS

A. Mode pairs investigated

This work considers three different mode pairs: a symmetric mode pair s1-s2 and two anti-symmetric mode pairs a1-a2 and a2-a4, as shown in Fig. 1 (the dispersion curves for phase and group velocities in an Al 6061 T6 plate). The s1-s2 mode pair with a phase velocity equal to the longitudinal velocity ($c_L = 6320$ m/s) satisfies all three conditions for the cumulative second harmonic generation. The two anti-symmetric mode pairs have a phase velocity $c_p = \sqrt{2}c_T$ and a group velocity $c_g = \sqrt{2}/2c_T$ (in which c_T is the shear velocity of the plate) and are known as Lamé modes.[18,20] These modes have only out-of-plane displacement (and zero in-plane displacement) components and thus are experimentally advantageous, especially for the liquid-coupled wedge transducers used in this research. However, all Lamé modes satisfy the phase and group velocity matching conditions, but not the excitability condition.[11,20] The fundamental and second harmonic frequencies, in terms of frequency times the plate thickness h, are $fh = 3.63$ MHz mm and 7.26 MHz mm for the s1-s2 mode pair, $fh = 4.43$ MHz mm and 8.86 MHz mm for the a1-a2 mode pair, and $fh = 8.86$ MHz mm and 17.72 MHz mm for the a2-a4 mode pair, as shown in Fig. 1.

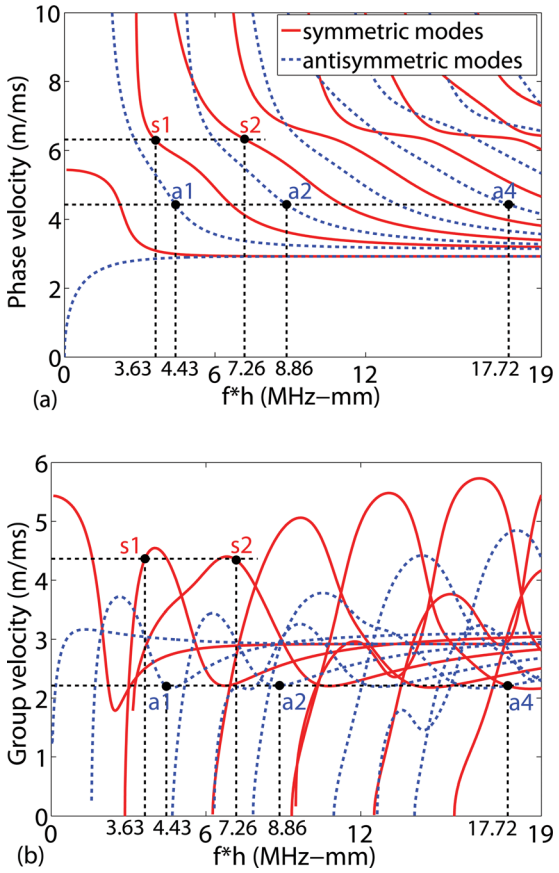

FIG. 1. (Color online) Dispersion curves for (a) phase velocity and (b) group velocity of an aluminum 6061 T6 plate.

The mode pairs selected are examined for their efficiency in characterizing the inherent material nonlinearity of undamaged aluminum plates. Previous investigations[1,3,7,8] on the nonlinear characteristics of longitudinal and Rayleigh waves used a normalized second harmonic amplitude A_2/A_1^2 versus the propagation distance (often called β') as a relative or uncorrected acoustic nonlinearity parameter, in which A_1 and A_2 are the amplitudes of the fundamental and second harmonic waves, respectively. Note that A_2/A_1^2 is proportional to the absolute acoustic nonlinearity parameter β and contains all the essential information needed to measure material nonlinearity. In order to compare the efficiency of the second harmonic generation of Lamb wave mode pairs at different frequencies and phase velocities (Fig. 1), the influences of the frequency and phase velocity on the nonlinearity parameter must be taken into account. Because there is no explicit expression available for the absolute nonlinearity parameter β in terms of surface displacements for Lamb waves, this research hypothesizes the following proportionality:

$$\beta \propto \frac{1}{z}\frac{c_p^2}{\omega^2}\frac{A_2}{A_1^2}, \tag{3}$$

where the right-hand side term is taken as the uncorrected (or relative) nonlinearity parameter β' for Lamb waves. This work then measures the normalized second harmonic amplitude $c_p^2 A_2/A_1^2\omega^2$ as a function of the propagation distance z. Thus, the slope in the plot of $c_p^2 A_2/A_1^2\omega^2$ versus z is the relative nonlinearity parameter β'.

B. Measurement setup

A schematic of the measurement setup is shown in Fig. 2. Four aluminum plates, two Al 6061 T6 plates and two Al 1100 H14 plates with a thickness h of either 1.6 mm or 3.175 mm, are used in the experiments. Lamb waves are generated and detected using variable-angle Plexiglas wedge transducers in the pitch-catch mode as shown in Fig. 2. The incident angle θ used to excite a specific Lamb mode is determined by Snell's law. A tone burst signal of 30 cycles at the fundamental frequency is generated by a high power gated amplifier (RITEC RAM-5000 Mark IV) and fed into the transmitter (KB-Aerotech Gamma C07416, with a center frequency of 2.25 MHz) for excitation of the targeted fundamental Lamb mode. The receiver (Panametrics A405S, with a center frequency of 5 MHz) simultaneously detects both fundamental and second harmonic waves. The wedge transducer assemblies are coupled to the specimen with light lubrication oil that produces a low level of variability in the second harmonic signals.[14] The measured time-domain signals are sampled at 100 MHz by an oscilloscope, averaged 1000 times to improve the signal-to-noise ratio, and then transferred to a computer for signal processing. All of the measurements are taken in the far field of the transducer[21] with a propagation distance of 22.5 cm to 45 cm in increments of 2.5 cm. At each propagation distance, three different measurements are taken in order to evaluate the experimental consistency. For each of these three measurements, the receiving wedge transducer assembly is completely removed and then reattached, whereas the transmitter remains unchanged. Care should be taken to ensure experimental consistency, including the same clamping force on the wedges for consistent coupling, the same instrumentation including transducers, and consistent signal processing parameters for all four different specimens. This is especially important when making an objective comparison of results from different mode pairs.

C. Signal processing of nonlinear Lamb waves

An accurate determination of both fundamental and second harmonic amplitudes from a measured time-domain

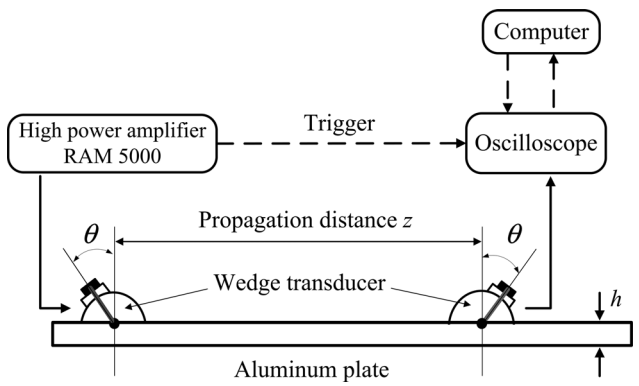

FIG. 2. Schematic of the experimental setup.

signal can be difficult when multiple modes are excited; other unwanted modes can contribute to the amplitudes of the fundamental and second harmonic amplitudes. In addition, the amplitude of the second harmonic wave is usually much smaller than that of the fundamental wave.[7,8,13,14] Therefore, a consistent and robust signal processing procedure is needed in order to correctly identify the amplitudes of the fundamental and second harmonics. Some researchers have used a method based on the short-time Fourier transform[1,7,14,17] to extract these amplitudes. However, the accuracy of this approach can be dependent on the user's experience in determining critical parameters such as the type, length, and overlap percentage of the window function. A set of inappropriate parameters can cause inaccurate results in the fundamental and second harmonic amplitudes, thus providing an unreliable prediction of the nonlinearity parameter.[14,22] This work employs the Morlet wavelet, which has shown to be robust in extracting these amplitude features from dispersive and multimode guided wave signals.[23–25] An advantage of this approach is that the amplitudes at the fundamental and second harmonic frequencies can be extracted (with the Morlet wavelet) without any user's optimization of the signal processing parameters.

The application of the Morlet wavelet relies on the fact that the peak magnitude of the wavelet coefficient at a frequency ω, $W(\omega)$, represents the wave component that propagates with a group velocity c_g at this frequency. This peak magnitude is proportional to the amplitude of the raw signal $A(\omega)$,[23]

$$W(\omega) = C(\omega)A(\omega), \tag{4}$$

where $C(\omega)$ is a frequency-dependent factor. In order to accurately compare the responses of the three mode pairs with different excitation frequencies, the amplitudes at both the fundamental (ω) and second harmonic (2ω) frequencies must be calibrated from their wavelet coefficients, i.e., $A_1 = W(\omega)/C(\omega)$ and $A_2 = W(2\omega)/C(2\omega)$.

Typical time-domain signals of the symmetric (s1-s2) and anti-symmetric (a1-a2) mode pairs measured at a propagation distance $z = 35$ cm in a 1.6-mm-thick Al 6061 plate and the associated wavelet coefficients at the fundamental and second harmonic frequencies are shown in Fig. 3 and Fig. 4. As both the s1 (at ω) and s2 (at 2ω) modes have the fastest group velocity (as seen in Fig. 1) in the excited frequency band, they correspond to the first peaks in the extracted components (Fig. 3(b)). It is seen that both s1 and s2 modes are well separated from the other simultaneously excited modes; thus their amplitudes can be accurately extracted. For the a1-a2 mode pair, it is clear in Fig. 4(a) that the a1 mode is dominant in the time domain signal relative to the other modes possibly excited. This is because the Lamé modes have only an out-of-plane displacement component and thus can easily be excited and detected with fluid-coupled wedge transducers. For this reason, the amplitudes of the harmonic components can be accurately extracted from the Morlet wavelet coefficients at the fundamental and second harmonic frequencies (Fig. 4(b)), even though their group velocity is not the fastest.

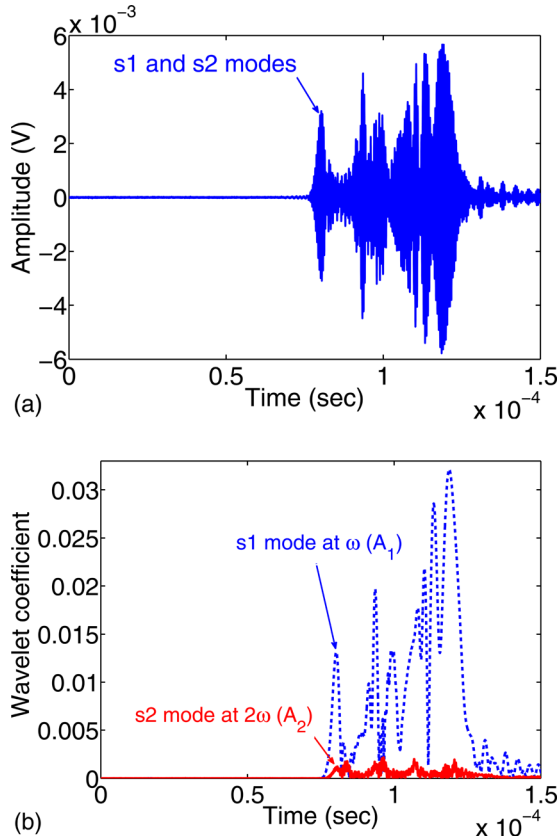

FIG. 3. (Color online) Representative results of (a) a typical time-domain signal of an s1-s2 mode pair measured at a propagation distance of z = 35 cm and (b) amplitude components of the fundamental and second harmonic frequencies extracted by the Morlet wavelet.

IV. RESULTS AND DISCUSSION

The normalized second harmonic amplitudes, $c_p^2 A_2/A_1^2\omega^2$ for the three mode pairs measured at ten propagation distances in the Al 6061 plates are shown in Fig. 5. Note that the initial value of $c_p^2 A_2/A_1^2\omega^2$ measured at the first distance, $z_0 = 22.5$ cm, has been subtracted from the rest of the results of each mode pair for comparison purposes. This initial value represents the nonlinearity of the measurement setup (electronics and transducers) and is constant for a given experimental setup; however, its value can vary with coupling conditions. The error bars indicate the standard deviation of the three different measurements that are repeated at each propagation distance, and this deviation is mainly attributed to coupling variability. The measured $c_p^2 A_2/A_1^2\omega^2$ for the s1-s2 mode pair shows a linear increase with propagation distance, and previous experimental work[1,13,14] has shown that this increase is due to material nonlinearity. Thus the experimental procedure used in this research appears to be reliable for characterizing second harmonic generation. It is surprising to observe in Fig. 5 that the normalized second harmonic amplitude of the anti-symmetric mode pairs (a1-a2 and a2-a4) also shows a linear increase with propagation distance. However, the slopes of these modes are significantly smaller than that of the s1-s2 mode pair (so that their fit lines look flat in Fig. 5): the slope of the a1-a2 mode pair is 71.7 times smaller than that of the s1-s2 mode pair, and the slope of the a2-a4 mode pair is 209.1 times smaller than that of the s1-s2

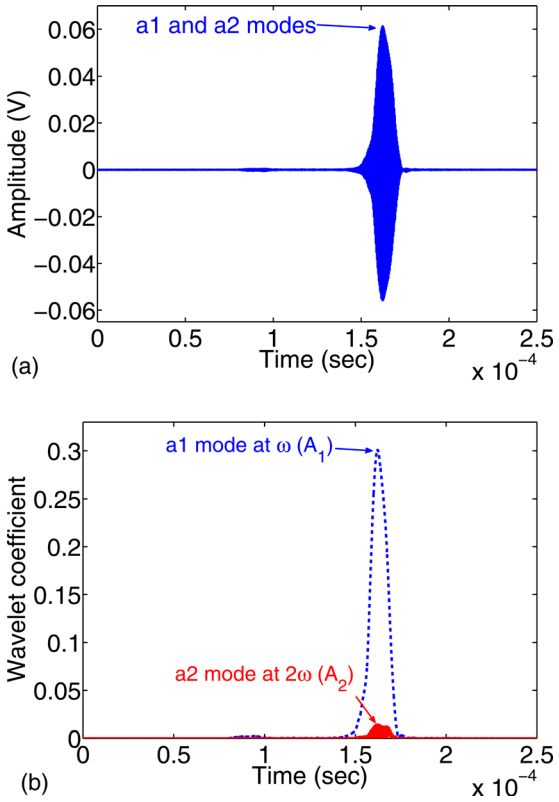

FIG. 4. (Color online) Representative results of (a) a typical time-domain signal of an a1-a2 mode pair measured at a propagation distance of z = 35 cm and (b) amplitude components of the fundamental and second harmonic frequencies extracted by the Morlet wavelet.

mode pair. Due to their negligibly small slopes (as compared to the s1-s2 mode pair), the anti-symmetric mode pairs will be very inefficient in experimentally characterizing material nonlinearity.

Whereas the theory of Ref. 11 predicts a zero slope for an anti-symmetric second harmonic Lamb mode due to the vanishing power flux, the experimental results in Fig. 5 show small but linear increases in the normalized second harmonic amplitude for the anti-symmetric mode pairs. Thus questions arise as to what contributes to these small linear increases, and whether they are due to cumulative second harmonic generation caused by the material nonlinearity. In order to investigate this, further measurements for both the a1-a2 and a2-a4 mode pairs are conducted on two aluminum plates (Al 6061 T6 and Al 1100 H14) that have different levels of material nonlinearity, again under the same experimental conditions. The ratio between the absolute nonlinearity parameters of these two materials measured with longitudinal waves[26] is $\beta_{\mathrm{Al}\,100}/\beta_{\mathrm{Al}\,6061} = 2.12$, and the ratio between the relative nonlinearity parameters measured on these two plates with the s1-s2 Lamb mode pair[13] is $\beta'_{\mathrm{Al}\,100}/\beta'_{\mathrm{Al}\,6061} = 2.77$. Therefore, the small linear increases for the anti-symmetric mode pairs can be attributed to the material nonlinearity only if the ratio between the slopes measured from these two different materials is close to 2.12. First, the ratio is calculated from the slopes measured with the a1-a2 mode pair for these two materials, and then, to double-check this measured ratio, measurements are performed with the a2-a4 mode pair. Figure 6 shows the normalized second harmonic amplitude for the a1-a2 and a2-a4 mode pairs in these two materials. It is interesting to note that both ratios are quite close to unity (1.12 for the a1-a2 mode pair and 1.05 for the a2-a4 mode pair). More interesting is the fact that these two ratios are very close to each other. The consistency in these results indicates that the linear increases with small slopes in the results for the a1-a2 and a2-a4 mode pairs are not due to the cumulative propagation of second harmonic waves. One possible cause for these small but measureable slopes is a

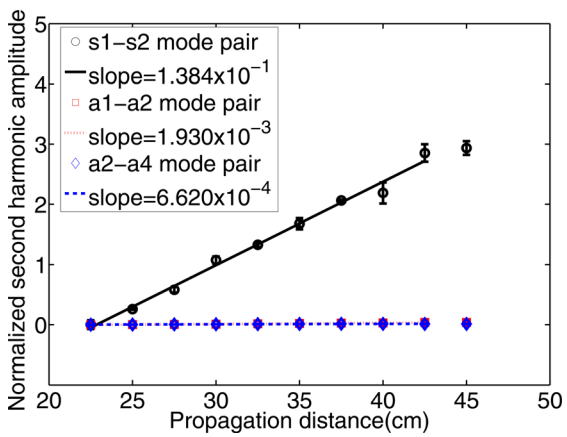

FIG. 5. (Color online) Comparison of the measured $c_p^2 A_2/A_1^2\omega^2$ vs the propagation distance for the s1-s2, a1-a2, and a2-a4 mode pairs in Al 6061-T6 plates.

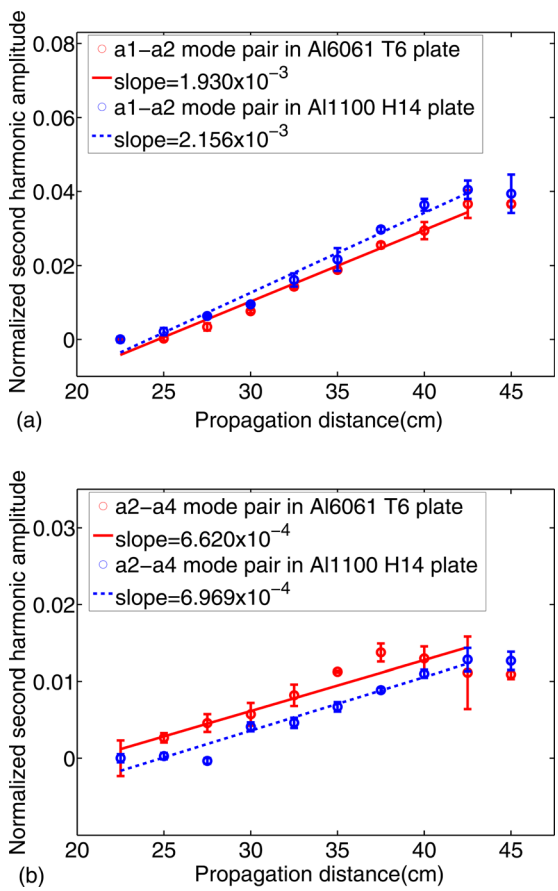

FIG. 6. (Color online) Comparison of the measured $c_p^2 A_2/A_1^2\omega^2$ vs the propagation distance for the (a) a1-a2 mode pair and (b) a2-a4 mode pair in an Al 6061-T6 plate and an Al 1100-H14 plate.

violation of the assumption of plane waves in the theory; this experimental setup generates wave fronts that are closer to cylindrical, as opposed to perfect plane waves. Clearly, further investigation is needed in order to completely understand the exact causes of these small slopes, but this is out of the scope of the present research.

V. CONCLUSIONS

This research experimentally investigates the symmetry properties of second harmonic Lamb waves by examining two anti-symmetric Lamé mode pairs (a1-a2 and a2-a4) and a symmetric mode pair (s1-s2) under the same experimental conditions. The s1-s2 mode pair with the longitudinal velocity theoretically satisfies all three conditions for cumulative second harmonic generation, whereas the a1-a2 and a2-a4 mode pairs satisfy only the phase and group velocity matching conditions. The three mode pairs are first examined in Al 6061 plates, and the experimentally measured normalized second harmonic amplitudes of all three mode pairs increase linearly with propagation distance. However, the slopes of the anti-symmetric mode pairs (a1-a2 and a2-a4) are two to three orders of magnitude smaller than that of the s1-s2 mode pair. Because the theory of Ref. 11 predicts a zero slope for the anti-symmetric mode pairs, further research investigates whether these small slopes are due to material nonlinearity. The same measurements are repeated on two plates with different levels of material nonlinearity, and the results show that the slopes of the two anti-symmetric mode pairs in two different materials are the same, which indicates that the measured slopes are not due to the material nonlinearity (or the cumulative second harmonic propagation). This research, therefore, experimentally proves that second harmonic generation does not occur in anti-symmetric Lamb wave modes, which is consistent with the theoretical prediction of the nonexistence of a second harmonic anti-symmetric Lamb wave mode.

ACKNOWLEDGMENTS

Yu Liu was financially supported by the China Scholarship Council (No. 2010601198) during her visit at the Georgia Institute of Technology.

[1]C. Pruell, J.-Y. Kim, J. Qu, and L. J. Jacobs, Appl. Phys. Lett. **91**, 231911 (2007).
[2]M. Deng and J. Pei, Appl. Phys. Lett. **90**, 121902 (2007).
[3]C. Pruell, J.-Y. Kim, J. Qu, and L. J. Jacobs, Smart Mater. Struct. **18**, 035003 (2009).
[4]Y. Xiang, M. Deng, F.-Z. Xuan, and C.-J. Liu, Ultrasonics **51**, 974 (2011).
[5]A. I. Korobov and M. Y. Izosimova, Acoust. Phys. **52**, 683 (2005).
[6]J. H. Cantrell and W. T. Yost, Int. J. Fatigue **23**, S487 (2001).
[7]J.-Y. Kim, L. J. Jacobs, J. Qu, and J. W. Littles, J. Acoust. Soc. Am. **120**, 1266 (2006).
[8]J. Herrmann, J.-Y. Kim, L. J. Jacobs, J. Qu, J. W. Littles, and M. F. Svage, J. Appl. Phys. **99**, 124913 (2006); M. Liu, J.-Y. Kim, J. Qu, and L. J. Jacobs, NDT & E Int. **44**, 67 (2011).
[9]M. Deng, J. Appl. Phys. **94**, 4152 (2003).
[10]M. Deng, J. Appl. Phys. **85**, 3051 (1999).
[11]M. F. Müller, J.-Y. Kim, J. Qu, and L. J. Jacobs, J. Acoust. Soc. Am. **127**, 2141 (2011).
[12]A. Srivastava and F. L. di Scalea, J. Sound Vib. **323**, 932 (2009).
[13]C. Bermes, J.-Y. Kim, J. Qu, and L. J. Jacobs, Appl. Phys. Lett. **90**, 021901 (2007).
[14]K. H. Matlack, J.-Y. Kim, L. J. Jacobs, and J. Qu, J. Appl. Phys. **109**, 014905 (2011).
[15]M. Deng, P. Wang, and X. Lv, J. Phys. D: Appl. Phys. **38**, 344 (2005).
[16]W. J. de Lima and M. F. Hamilton, J. Sound Vib. **265**, 819 (2003).
[17]T.-H. Lee, I.-H. Choi, and K.-Y. Jhang, Mod. Phys. Lett. **22B**, 1135 (2008).
[18]N. Matsuda and S. Biwa, J. Appl. Phys. **109**, 094903 (2011).
[19]M. Deng, Y. Xiang, and L. Liu, J. Appl. Phys. **109**, 113525 (2011).
[20]K. F. Graff, *Wave Motion in Elastic Solids* (Oxford University Press, London, 1975).
[21]A. Ruiz and P. B. Nagy, J. Acoust. Soc. Am. **112**, 835 (2002).
[22]C. Pruell, J.-Y. Kim, J. Qu, and L. J. Jacobs, NDT & E Int. **42**, 199 (2009).
[23]Y. Liu, Z. Li, and W. Zhang, Nondestr. Test. Eval. **25**, 25 (2010).
[24]J. Lin and L. S. Qu, J. Sound Vib. **234**, 135 (2000).
[25]K. Kishimoto, H. Inoue, and M. Hamada, J. Appl. Mech. **62**, 841 (1995).
[26]W. T. Yost and J. H. Cantrell, in *Review of Progress in Quantitative Nondestructive Evaluation*, edited by D. O. Thompson and D. E. Chimenti (Plenum, New York, 1993), pp. 2067-2073.